JCM
Journals.ASM.org

Clonal Diversification and Changes in Lipid Traits and Colony Morphology in *Mycobacterium abscessus* Clinical Isolates

In Kwon Park,[a] Amy P. Hsu,[a] Hervé Tettelin,[b] Shamira J. Shallom,[c] Steven K. Drake,[d] Li Ding,[a] Un-In Wu,[a]* Nick Adamo,[a] D. Rebecca Prevots,[a] Kenneth N. Olivier,[e] Steven M. Holland,[a] Elizabeth P. Sampaio,[a,f] Adrian M. Zelazny[a,c]

Laboratory of Clinical Infectious Diseases, National Institute of Allergy and Infectious Diseases, National Institutes of Health, Bethesda, Maryland, USA[a]; Institute for Genome Sciences, University of Maryland School of Medicine, Baltimore, Maryland, USA[b]; Microbiology Service, Department of Laboratory Medicine, Clinical Center, National Institutes of Health, Bethesda, Maryland, USA[c]; Critical Care Medicine Department, Clinical Center; National Institutes of Health, Bethesda, Maryland, USA[d]; Pulmonary Clinical Medicine Section, Cardiovascular and Pulmonary Branch, National Heart, Lung, and Blood Institute, National Institutes of Health, Bethesda, Maryland, USA[e]; Leprosy Laboratory, Oswaldo Cruz Institute, FIOCRUZ, Rio de Janeiro, Brazil[f]

The smooth-to-rough colony morphology shift in *Mycobacterium abscessus* has been implicated in loss of glycopeptidolipid (GPL), increased pathogenicity, and clinical decline in cystic fibrosis (CF) patients. However, the evolutionary phenotypic and genetic changes remain obscure. Serial isolates from nine non-CF patients with persistent *M. abscessus* infection were characterized by colony morphology, lipid profile via thin-layer chromatography and matrix-assisted laser desorption ionization–time of flight mass spectrometry (MALDI-TOF MS), sequencing of eight genes in the GPL locus, and expression level of *fadD23*, a key gene involved in the biosynthesis of complex lipids. All 50 isolates were typed as *M. abscessus* subspecies *abscessus* and were clonally related within each patient. Rough isolates, all lacking GPL, predominated at later disease stages, some showing variation within rough morphology. While most (77%) rough isolates harbored detrimental mutations in *mps1* and *mps2*, 13% displayed previously unreported mutations in *mmpL4a* and *mmpS4*, the latter yielding a putative GPL precursor. Two isolates showed no deleterious mutations in any of the eight genes sequenced. Mixed populations harboring different GPL locus mutations were detected in 5 patients, demonstrating clonal diversification, which was likely overlooked by conventional acid-fast bacillus (AFB) culture methods. Our work highlights applications of MALDI-TOF MS beyond identification, focusing on mycobacterial lipids relevant in virulence and adaptation. Later isolates displayed accumulation of triacylglycerol and reduced expression of *fadD23*, sometimes preceding rough colony onset. Our results indicate that clonal diversification and a shift in lipid metabolism, including the loss of GPL, occur during chronic lung infection with *M. abscessus*. GPL loss alone may not account for all traits associated with rough morphology.

Organisms within the so-called *Mycobacterium abscessus* complex (MABSC) belong to the rapidly growing mycobacteria. Increasing evidence supports the division of MABSC into three related subspecies: *M. abscessus* subspecies *abscessus* (here referred as *M. abscessus*), *M. abscessus* subspecies *massiliense*, and *M. abscessus* subspecies *bolletii* (1–5).

MABSC causes serious chronic pulmonary infections in those with underlying conditions such as bronchiectasis or cystic fibrosis (CF). In the United States and some other parts of the world, it is the second most frequent pulmonary nontuberculous mycobacterial (NTM) infection (28%), after *Mycobacterium avium* complex, and its prevalence is increasing (6, 7). MABSC causes significant mortality in the CF population. In Scandinavian countries, one-fourth of CF patients who have persistently positive MABSC sputum cultures have received lung transplantation or died (8).

Glycopeptidolipid (GPL) is the most abundant glycolipid in the outer cell envelope of MABSC, and its synthesis and transport are controlled by the GPL locus (9). A growing number of studies have linked the rough colony morphology in MABSC to loss of GPL, increased pathogenicity, and clinical decline in CF patients (10–16). While most studies of persistent MABSC infection focused on CF patients, less is known about MABSC in the non-CF population regarding presence of mixed populations, clonal relatedness, and phenotypic and genotypic changes of strains collected over time.

We have very limited understanding of the evolutionary phenotypic and genetic changes occurring in MABSC during persistent human lung infection. We lack the fundamental knowledge needed to identify selective pressures associated with rough morphology and, once identified, how to reverse them. To address these questions, we collected serial clinical isolates of *M. abscessus* from non-CF patients with persistent pulmonary infection who were followed for 5 years or more and assessed strain relatedness and diversity, colony morphology, lipid profiles, mutations in GPL locus genes, and lipid metabolism.

Received 24 July 2015 **Accepted** 29 July 2015

Accepted manuscript posted online 19 August 2015

Citation Park IK, Hsu AP, Tettelin H, Shallom SJ, Drake SK, Ding L, Wu U-I, Adamo N, Prevots DR, Olivier KN, Holland SM, Sampaio EP, Zelazny AM. 2015. Clonal diversification and changes in lipid traits and colony morphology in *Mycobacterium abscessus* clinical isolates. J Clin Microbiol 53:3438–3447. doi:10.1128/JCM.02015-15.

Editor: B. A. Forbes

Address correspondence to Adrian M. Zelazny, azelazny@mail.nih.gov.

* Present address: Un-In Wu, National Taiwan University Hospital, Department of Internal Medicine, Taipei, Taiwan.

Supplemental material for this article may be found at http://dx.doi.org/10.1128/JCM.02015-15.

TABLE 1 Patient demographics

Patient	Age (yr)	Gender	Underlying disease	Duration (yr)[a]	Persistence of positive acid-fast bacillus smears	Living/deceased	No. of isolates[b]
1	74	Female	NTM disease with idiopathic bronchiectasis (non-CF)	12	Persistent	Living	8
2	79	Male	NTM disease with idiopathic bronchiectasis (non-CF but CF carrier)	10	Persistent	Living	2
3	54	Female	Interferon gamma autoantibodies, disseminated disease	10	Persistent	Living	3
4	61	Female	NTM disease with idiopathic bronchiectasis (non-CF)	9	Persistent	Living	12
5	77	Female	NTM disease with idiopathic bronchiectasis (non-CF)	7	Persistent	Deceased	5
6	69	Female	NTM disease with idiopathic bronchiectasis (non-CF but CF carrier)	7	Persistent	Deceased	4
7	70	Female	NTM disease with idiopathic bronchiectasis (non-CF)	8	Persistent	Living	8
8	87	Female	NTM disease with idiopathic bronchiectasis (non-CF)	5	Persistent	Deceased	2
9	82	Male	NTM disease with idiopathic bronchiectasis (non-CF)	8	Persistent	Living	6

[a] Interval between the first and last serial isolates.
[b] The number of available isolates varied among the patients.

MATERIALS AND METHODS

Mycobacterial isolates and culture. The clinical isolates were kept at −80°C in Tween-albumin broth (Remel, Lenexa, KS) at the Microbiology Service of the NIH Clinical Center. Each isolate was labeled with patient number, chronological isolate number, and colony morphology [e.g., the third isolate from patient 6 with rough morphology is 6-3(R)]. Prior to use, the isolates were cultured on Middlebrook 7H11 agar plates at 37°C for 3 to 5 days. For experiments requiring growth in liquid medium, colonies were inoculated into Middlebrook 7H9 broth supplemented with albumin, dextrose, and catalase (ADC) with 0.05% Tween 80.

Microscopy. Pictures of colonies were taken after 72 to 96 h of incubation at 37°C on 7H11 agar plates using a light microscope (Nikon Eclipse 50i) equipped with a camera (Olympus DP70) at a magnification of ×100.

DNA extraction from mycobacterial isolates. DNA was extracted from each isolate by use of the Mo Bio Ultra Clean microbial DNA isolation kit (Mo Bio Laboratories, Carlsbad, CA) according to the manufacturer's instructions.

Sequencing of 8 GPL locus genes. Whole-genome sequencing (WGS) of mycobacteria was previously done on the 19 isolates from patients 1, 7, and 9. These isolates were 1-2(S) to 1-7(S), 7-1(S) to 7-4(R) and 7-6(S) to 7-8(R), 9-1(S) to 9-6(R) (see Table S1 in the supplemental material for NCBI accession numbers). Discrete gene sequences were obtained from the WGS data. The remaining 31 isolates were subjected to targeted sequencing of 8 genes in the GPL locus as described below.

Amplification of the genes of interest was performed using Platinum *Taq* Hi-Fidelity Supermix (Life Technologies, Carlsbad, CA) per the manufacturer's instructions. The primers were chosen based on the reference genome of *M. abscessus* ATCC 19977^T available in NCBI (see Table S2 in the supplemental material). The resulting PCR products were treated with ExoSAP-IT (Affymetrix, Santa Clara, CA) and sequenced using BigDye v3.1 Ready Reaction mix (Life Technologies). Reaction products were purified using DTR Performa spin plates (Edge BioSystems, Gaithersburg, MD) and run on a 3730XL DNA Analyzer (Life Technologies). Chromatograms were aligned and analyzed using Sequencher (Gene Codes, Ann Arbor, MI).

Multilocus genotyping of the clinical isolates. Primers were chosen based on previously reported multilocus sequence typing (MLST) schemes (3, 5) (see Table S2 in the supplemental material). Following PCR amplification and sequencing, partial sequences of the 3 housekeeping genes *hsp65*, *secA*, and *rpoB* from each genome were concatenated. For the 19 isolates that underwent WGS previously, sequences were obtained from the WGS data. The concatenated sequences were aligned by the ClustalW algorithm and used for construction of a neighbor-joining phylogenetic tree by MEGA software.

Extraction of crude GPL from *M. abscessus* clinical isolates and TLC. Crude GPL was extracted as previously described (17). Briefly, strains grown on the 7H11 agar plates were inoculated into 7H9 liquid medium supplemented with ADC. After growth for 72 to 96 h at 37°C with continuous shaking, optical densities at 600 nm (OD_{600}) were measured (DU-530 spectrophotometer; Beckman, Indianapolis, IN). Cultures were diluted with fresh 7H9 liquid medium to an OD_{600} of 0.025 and grown to logarithmic growth phase (OD_{600}, 0.6 to 0.9). After washing twice with phosphate-buffered saline (PBS), bacterial pellets were weighed to keep differences among serial isolates from a patient within 10% of each other. Pellets were resuspended in 2:1 chloroform-methanol (10 μl per mg wet pellet) and left overnight for lipid extraction. Following centrifugation, 2 μl of the supernatant containing extracted total unbound lipids was used for matrix-assisted laser desorption ionization–time of flight mass spectrometry (MALDI-TOF MS) (see below). For further extraction of crude GPL, 0.9% NaCl at 20% of the volume of the supernatant was added. After vortexing and centrifugation, the organic layer containing GPL (bottom) was separated from the aqueous layer (top) and left for complete evaporation of the solvent. Crude GPL extract was then resuspended in 20 μl of 2:1 chloroform-methanol, spotted on an analytical thin-layer chromatography (TLC) plate (Silica Gel 60; EMD Millipore, Germany), and run in 100:7 chloroform-methanol, followed by spraying with 0.1% orcinol in 40% H_2SO_4 and charring at 140°C for visualization.

MALDI-TOF MS of lipid extracts. The total unbound lipid extracts from before the biphasic separation were subjected to MALDI-TOF MS. Two microliters of the lipid extract was dried on a steel MALDI-TOF MS sample target on a heat plate at 45°C. This was overlain with the matrix solution (1 μl of saturated α-cyano-4-hydroxycinnamic acid [CHCA] in

50% acetonitrile, 2.5% trifluoroacetic acid [TFA]), and 47.5% water). The Bruker autoflex MALDI-TOF MS system (Bruker, Billerica, MA) was calibrated across the relevant range, and spectra were collected in positive reflectron mode.

Normalization of the samples by copy numbers of the 16S rRNA gene. Prior to TLC of triacylglycerol (TAG) and RNA extraction, we normalized the liquid cultures following the previously reported methodologies for mycobacterial quantification based on quantitative PCR (qPCR) (18, 19). We chose to do qPCR of the 16S rRNA gene because it is highly conserved and only a single copy exists in the *M. abscessus* genome. After harvesting liquid cultures at an OD_{600} of 0.6 to 0.9, samples underwent water bath sonication (Aquawave 9374; Barnstead Lab-Line, Germany) with glass beads for 15 min to minimize clumping, followed by vigorous vortexing, and then 20 μl from each sample was lysed at 100°C for 15 min in a thermocycler. Absolute quantification of the 16S rRNA gene with an Applied Biosystems 7500 real-time PCR system (Grand Island, NY) was performed using 2 μl of the lysate along with 0.6 μM each primer (see Table S2 in the supplemental material), 21 μl of SYBR green PCR master mix (Applied Biosystems, Grand Island, NY), and 21 μl of water (total reaction volume, 50 μl). The initial holding stage was set to 95°C for 15 min, followed by 40 cycles of 1 min at 94°C and 1 min at 60°C. Fluorescence measurement was taken during the 60°C step in each cycle. Standard curves were generated using the purified PCR product from amplification of the 16S rRNA gene with the same primers and genomic DNA from a smooth *M. abscessus* clinical strain. The weight of the PCR product in 2 μl and its base pair length obtained from the 2100 Bioanalyzer system (Agilent Technologies, Santa Clara, CA) were converted to the number of copies of the 16S rRNA gene using the following formula: number of copies = (weight in ng × 6.022×10^{23})/(base pair length × 10^9 × 660), where the estimation for the weight of one base pair is 660 Da (QuantiTect SYBR; Qiagen [2002]).

TLC separation of TAG and detection by MALDI-TOF MS. A 250-μl portion of each liquid culture sample normalized by copy numbers of the 16S rRNA gene (10^8 copies per ml) underwent the crude lipid extraction as described above, followed by TLC for separation of triacylglycerol (TAG). The solvent system used was hexane-diethyl ether-acetic acid at 70:30:1 (20). After the run, the TLC plate was sprayed with 10% $CuSO_4$ in 10% phosphoric acid and charred at 110°C until the separated lipids were visualized (21).

Two separate plates, both loaded with the crude lipid extract from 1-8(R), underwent the TLC runs for TAG as described above simultaneously in the same tank. One plate was sprayed and charred for visualization, while the other was left intact. The silica in the band corresponding to TAG on the intact plate, in comparison to the visualized counterpart, was scraped off and washed with 2:1 chloroform-methanol. After centrifugation, the supernatant was subjected to MALDI-TOF MS as described above.

RNA extraction from the mycobacteria and conversion to cDNA. Liquid culture samples normalized by copy numbers of the 16S rRNA gene (10^8 copies per ml) were subjected to RNA isolation (Qiagen, 2006). The concentration of the extracted total RNA in ng/μl was measured with a NanoDrop ND-100 spectrophotometer (Thermo Scientific, Wilmington, DE). Twelve nanograms of the total RNA was converted to cDNA (SuperScript III quantitative reverse transcription-PCR [qRT-PCR]; Invitrogen, Grand Island, NY), following the manufacturer's instructions.

Measurement of cDNA copy numbers of *fadD23*. Absolute quantification with the Applied Biosystems 7500 real-time PCR system was performed using 4 μl of the cDNA sample from the step described above, 0.6 μM each primer targeting *fadD23* (see Table S2 in the supplemental material), 20 μl of SYBR green PCR master mix, and 20 μl of water in a total reaction volume of 50 μl. The initial holding stage was set to 95°C for 10 min, followed by 40 cycles of 15 s at 95°C and 1 min at 60°C. Fluorescence measurement was taken during the 60°C step in each cycle. Standard curves were generated as described above.

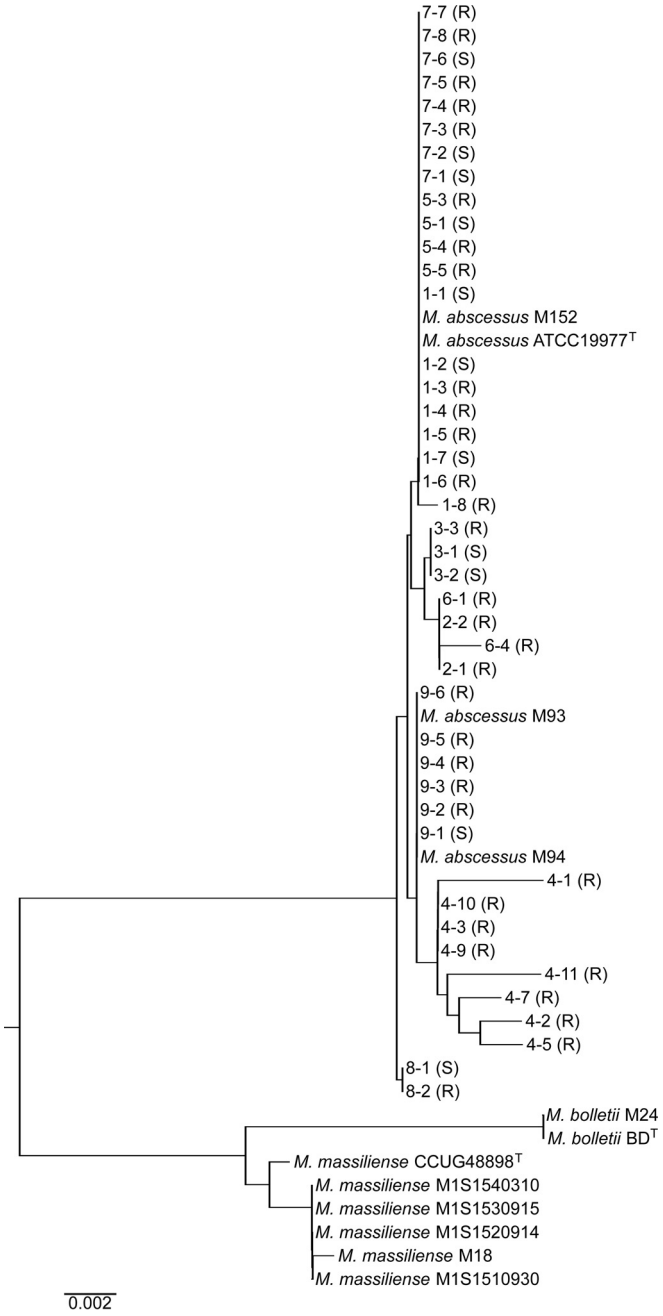

FIG 1 Phylogenetic tree based on MLST (concatenated *hsp65-secA-rpoB* sequences). The clinical isolates in this study clustered with other *M. abscessus* genomes available in NCBI, apart from *M. abscessus* subsp. *massiliense* or *M. abscessus* subsp. *bolletii*. The serial isolates from each patient showed shared evolutionary lineage, demonstrating their close genetic relatedness.

RESULTS

Patients. All available serial isolates from the non-CF patients with persistent *M. abscessus* pulmonary infection who were followed at the NIH Clinical Center for 5 years or more were included in the study (9 patients, total of 50 isolates). The median follow-up time was 8 years, with a maximum of 12 years.

The majority of patients (8 out of 9) had pulmonary NTM disease with idiopathic bronchiectasis. One had disseminated infection due to interferon gamma autoantibodies (Table 1).

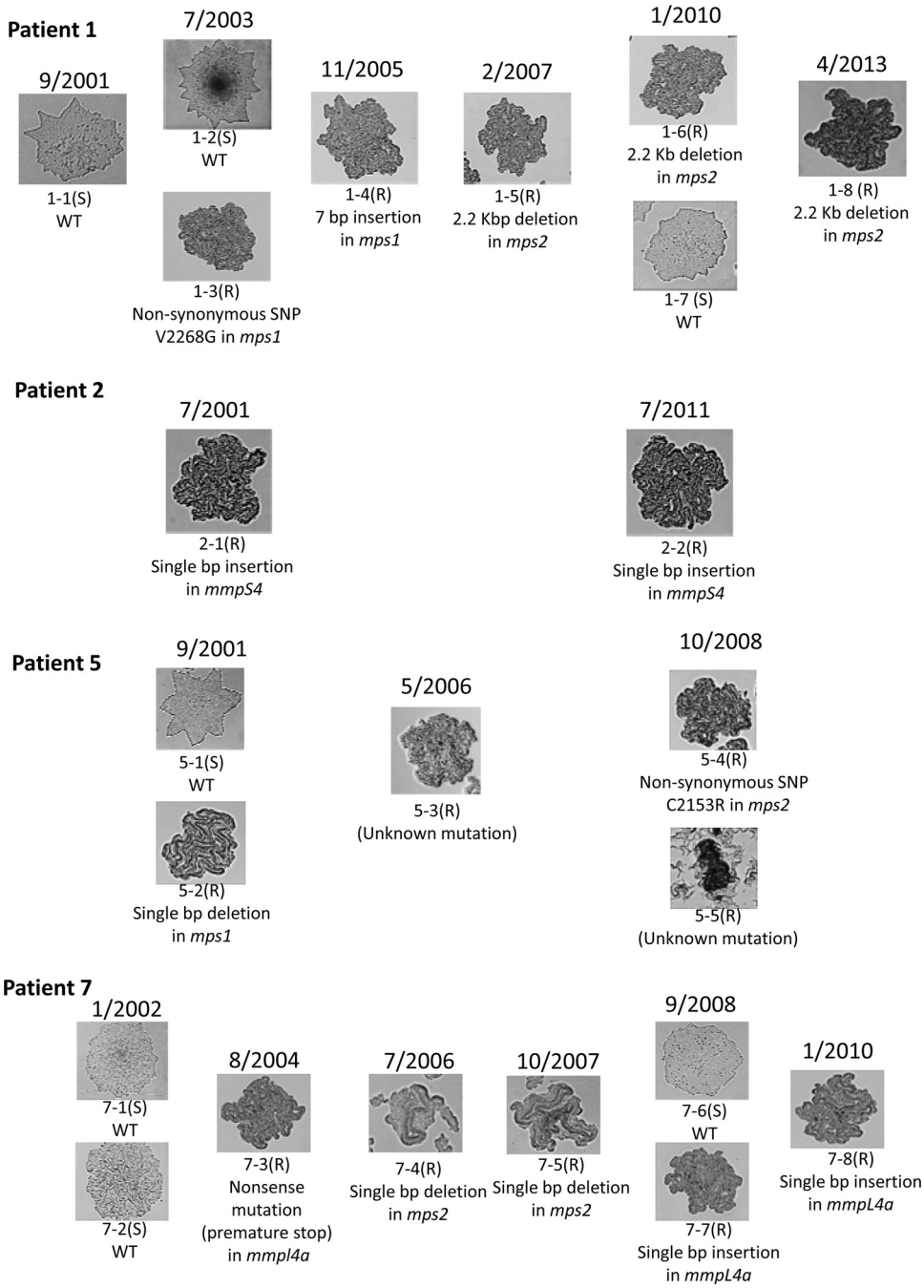

FIG 2 Representative single-colony pictures of the serial isolates from patients 1, 2, 5, and 7 at a magnification of ×100, displayed chronologically from left to right. The isolates obtained on the same date are shown in one column (single-colony pictures of the isolates from patients 3, 4, 6, 8, and 9 are shown in Fig. S1 in the supplemental material). WT, wild type; S, smooth; R, rough; SNP, single nucleotide polymorphism.

Phylogenetic analysis of the clinical isolates by MLST. Chronic infection with MABSC could potentially result from persistence of the initial strain and/or from reinfection with other strains. In order to differentiate between these two scenarios, all serial isolates were typed by a molecular method. Close genetic relatedness among serial isolates by patient is shown by the phylogenetic analysis based on multilocus sequence typing (MLST) using concatenated *hsp65*, *secA*, and *rpoB* sequences supporting strain persistence (3) (Fig. 1). Therefore, the changes observed among the serial isolates reflect adaptive processes of *M. abscessus* in response to chronic human lung infection.

Single-colony morphology. Smooth and rough colony morphotypes were assessed by microscopic inspection of isolates on 7H11 agar plates, (Fig. 2; see Fig. S1 in the supplemental material). In 6 out of the 9 patients, the colony morphology of the serial isolates was initially smooth before becoming predominantly rough. Serial isolates from the other 3 patients showed rough colony morphology throughout.

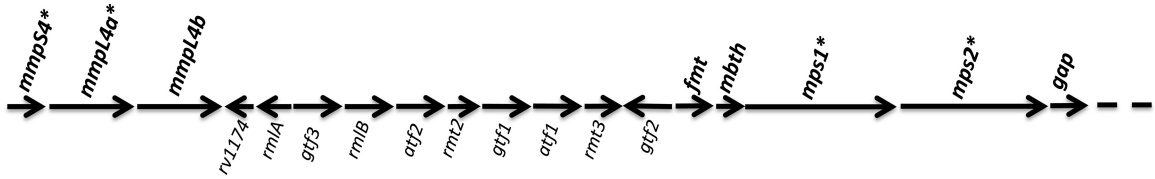

FIG 3 A segment of the GPL locus at the 5′ end in the *M. abscessus* genome, as described by Ripoll et al. (9). The genes in bold at the top are the 8 genes that underwent targeted sequencing in this study. We found a detrimental mutation in 4 of the 8 genes (*mmpS4*, *mmpL4a*, *mps1*, and *mps2* [*]) in 35 of the 39 rough clinical isolates included in the study. Most of these mutations were present in either in *mps1* or *mps2*, but the 3 rough isolates from patient 7 had detrimental mutations in *mmpL4a*, while the 2 rough isolates from patient 2 had them in *mmpS4*.

GPL locus mutations in the rough clinical isolates. We analyzed 8 genes in the GPL locus, including the genes in which spontaneous insertions/deletions (indels) were previously identified in rough *M. abscessus* clinical strains (*mps1* and *mmpL4b*) (22) as well as those which when experimentally rendered nonfunctional resulted in a switch from smooth to rough in *M. abscessus* or *M. smegmatis* (*gap*, *mps2*, *mbtH*, *mmpL4b*, and *mmpS4*) (17, 23–25). *fmt* and *mmpL4a* were included because of their adjacency to the above genes (Fig. 3). None of the 11 smooth isolates had a detrimental mutation in the 8 genes sequenced (in the entire GPL locus for those isolates with WGS data). Out of a total of 39 rough isolates, 35 (90%) had detrimental mutations, ranging from a single-base-pair indel to a 3.1-kbp deletion in *mps1-mps2* or *mmpS4-mmpL4a*. None of the 35 isolates had more than one detrimental mutation in the 8 genes (in the entire GPL locus for the isolates with WGS data). We also observed different GPL locus mutations within individual patients' isolates (patients 1, 4, 5, 7, and 9). For the remaining 4 rough isolates, 1-3(R) and 5-4(R) carried nonsynonymous SNPs with unclear consequences in *mps1* and *mps2*, respectively. Interestingly, no detrimental mutations in 5-3(R) or 5-5(R) were identified within the 8 genes sequenced (Table 2).

Overall, the majority of the detrimental GPL locus mutations in the rough clinical isolates occurred in the *mps1-mps2* segment (77% of the rough isolates). In 13% of the strains, changes were found in the *mmpS4-mmpL4a* segment. Mutations in *mmpS4-mmpL4a* have not been reported previously in spontaneously occurring rough strains of *M. abscessus*.

MALDI-TOF MS and TLC of the crude GPL extracts. We performed MALDI-TOF MS on the crude unbound lipid extracts from all 50 clinical isolates (Fig. 4; see Fig. S2 in the supplemental material). The isolates determined as smooth by microscopy had MALDI-TOF MS spectra that matched the previously published GPL spectrum of *M. abscessus* (9). On the other hand, none of the 39 rough isolates showed spectra of GPL; 37 had no spectrum in

TABLE 2 GPL locus mutations identified in the rough isolates

Patient	GPL locus mutation(s) in the rough isolates	Consequence
1	1-3(R), nonsynonymous SNP in *mps1*	V2268G
	1-4 (R), 7-bp insertion in *mps1* (2348_2354dup)	Frameshift
	1-5(R), 1-6(R), 1-8(R), 2.2-kbp deletion in *mps2* (3556_5801del)	Large deletion
2	2-1(R), 2-2(R), single-base-pair insertion in *mmpS4* (149_150insT)	Frameshift
3	3-3(R), single-base-pair insertion in *mps1* (4963_4964insG)	Frameshift
4	4-1(R), single-base-pair insertion in *mps1* (3240_3241insC)	Frameshift
	4-2(R), double-base-pair insertion in *mps2* (1621_1622insGG)	Frameshift
	4-3(R), 4-4(R), single-base-pair insertion in *mps1* (3240_3241insC)	Frameshift
	4-5(R), 4-6(R), double-base-pair insertion in *mps2* (1621_1622insGG)	Frameshift
	4-7(R), single-base-pair insertion in *mps1* (3240_3241insC)	Frameshift
	4-8(R), double-base-pair insertion in *mps2* (1621_1622insGG)	Frameshift
	4-9(R), 4-10(R), 4-11(R), 4-12(R), single-base-pair insertion in *mps1* (3240_3241insC)	Frameshift
5	5-2(R), single-base-pair deletion in *mps1* (8335delC)	Frameshift
	5-3(R), no mutation identified	
	5-4(R), nonsynonymous SNP in *mps2*	C2153R
	5-5(R), no mutation identified	
6	6-1(R), 6-2(R), 6-3(R), 6-4(R), single-base-pair deletion in *mps1* (5714delT)	Frameshift
7	7-3(R), nonsense mutation in *mmpl4a* (2206G→T)	Premature stop codon
	7-4(R), 7-5(R), single-base-pair deletion in *mps2* (266delC)	Frameshift
	7-7(R), 7-8(R), single-base-pair insertion in *mmpL4a* (269_270insG)	Frameshift
8	8-2(R), 3.1-kbp deletion spanning both *mps1* and *mps2* (*mps1* base 7481 through *mps2* base 192)	Large deletion
9	9-2(R), 9-3(R), 9-4(R), 9-5(R), single-base-pair insertion in *mps2* (5193_5194insG)	Frameshift
	9-6(R), single-base-pair insertion in *mps1* (5176_5177insG)	Frameshift

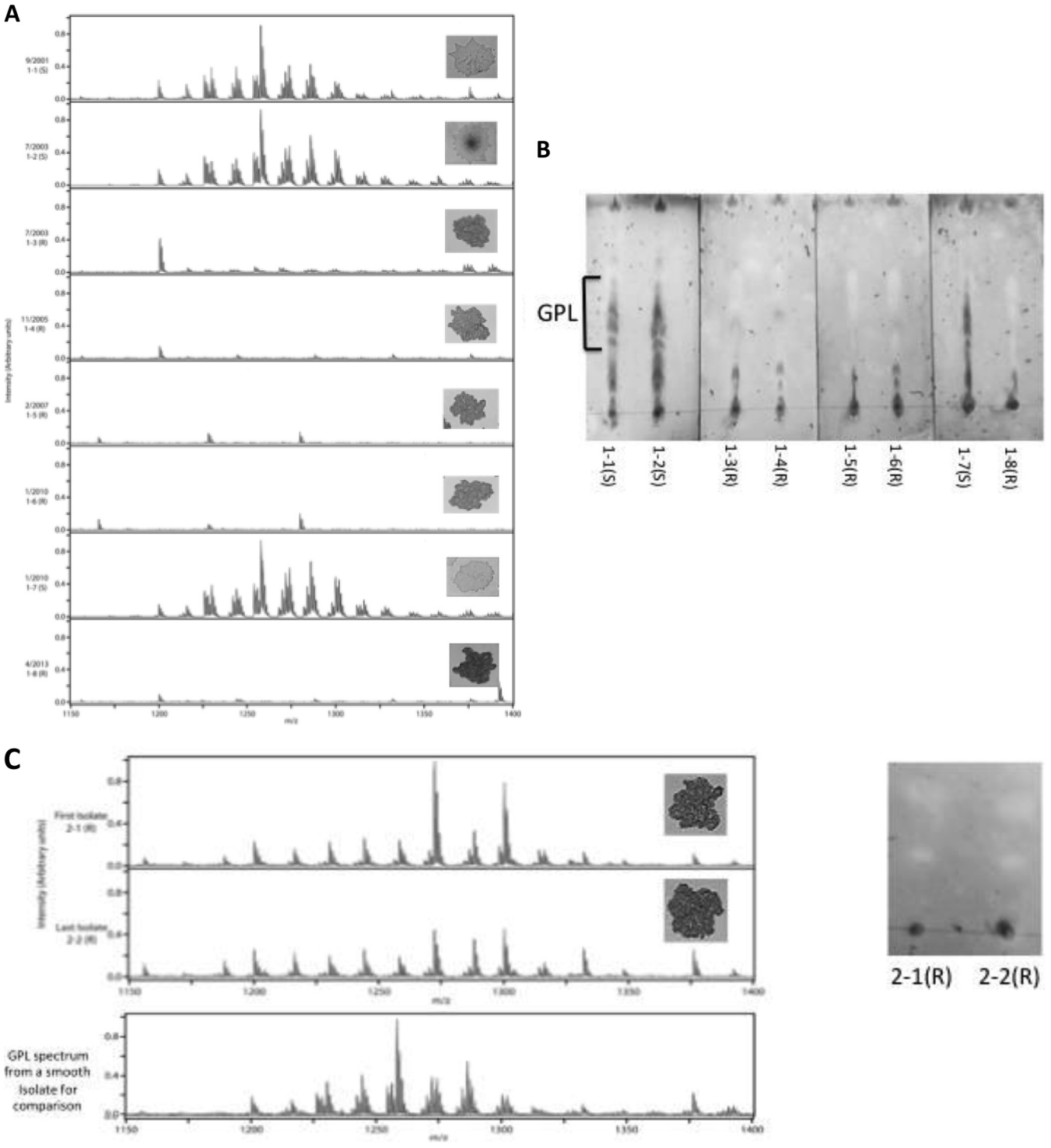

FIG 4 (A) MALDI-TOF MS of the lipid extracts from patient 1 isolates. The MALDI-TOF MS spectra corresponding to GPL are present only in the smooth isolates. This indicates complete absence of GPL in the rough isolates. (B) The TLC results also agreed with the findings of MALDI-TOF MS. (C) MALDI-TOF MS and TLC of the isolates from patient 2. The rough isolates from this patient were found to have mutations in *mmpS4*. Note that *mmpS4* mutants showed spectra in the molecular mass range where GPL is detected in MALDI-TOF MS, but the major peaks have atomic mass values higher than those of GPL (whose spectrum is shown together for comparison). The TLC of the *mmps4* mutants did not show GPL bands. MALDI-TOF MS and TLC of the first and last isolates from patients 3, 4, 5, 6, 7, 8, and 9 are shown in Fig. S2 in the supplemental material. R, rough; S, smooth.

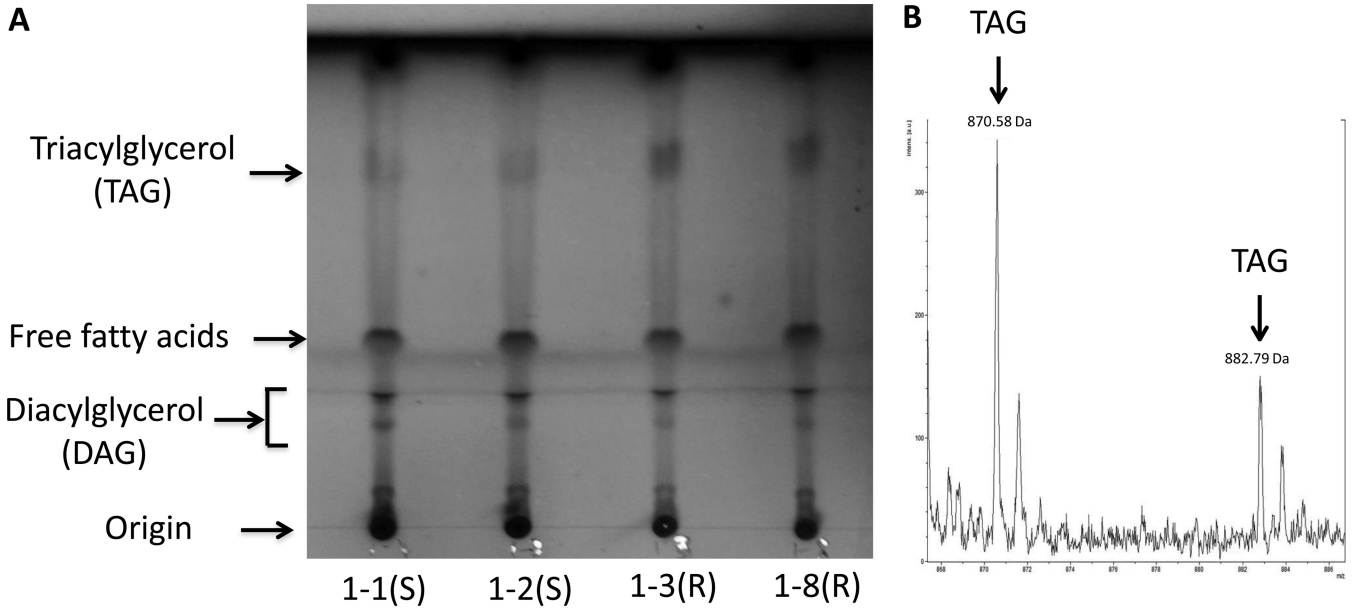

FIG 5 (A) The band corresponding to TAG becomes increasingly darker in the later clinical isolates, suggesting accumulation of TAG in *M. abscessus* as it gains persistence in the human lung. The solvent system used was hexane-diethyl ether-acetic acid at 70:30:1. Bands were visualized by spraying with 10% (wt/vol) $CuSO_4$ in 10% phosphoric acid, followed by charring at 110°C (20, 21). (B) MALDI-TOF MS of the lipid extract from the silica scraped off the band corresponding to TAG in the TLC run of 1-8(R). The peaks had molecular masses matching those of TAG in the Lipidomics Gateway database (http://www.lipidmaps.org) and were consistent with what has been reported in the literature on TAG in NTM species (30). R, rough; S, smooth.

the molecular mass range of GPL. Only two rough isolates, 2-1(R) and 2-2(R), with frameshift mutations in *mmpS4* had spectra in the GPL range, but their peaks had atomic mass values higher than those of GPL (Fig. 4). TLC on the extracts from all 39 rough isolates did not show bands corresponding to GPL.

Variation in rough morphology. Although the rough isolates were clearly distinguishable from the smooth isolates, there was significant variation in rough morphology. The rough colonies of serial isolates from patients 4, 5, and 6 (Fig. 2; see Fig. S1 in the supplemental material) became denser and more irregularly shaped in the later-disease isolates. This variation in rough morphology was independent of GPL locus mutation. For example, all patient 6 serial isolates were devoid of GPL and had the same single-base-pair deletion in *mps1* (5714delT), but they showed significant variation in rough morphology.

Accumulation of TAG in the later clinical isolates. The accumulation of triacylglycerol (TAG) and the downregulation of synthesis of complex lipids occur in *M. tuberculosis* in response to various stressors in the human lung, such as hypoxia and low pH, presumably enabling the use of host fatty acids and cholesterol for an energy source (26–29). To test if TAG accumulation occurs in *M. abscessus* during chronic human lung infection, we performed TLC to separate TAG, using the samples normalized by copy numbers of the 16S rRNA gene. The bands corresponding to TAG were darker on the TLC runs of the later-collected serial isolates (Fig. 5; see Fig. S3 in the supplemental material), suggesting accumulation of TAG in *M. abscessus* during infection of human lung. MALDI-TOF MS on the silica scraped from the TAG bands showed peaks that matched the molecular masses of TAG (Fig. 5) and were consistent with those reported previously (30).

Reduced expression of *fadD23*, which is involved in synthesis of complex lipids. *fadD23*, one of the *M. abscessus* genes in the GPL locus (9), encodes a fatty acyl-AMP ligase (FAAL) that activates long-chain fatty acids as acyl-adenylates, which are then further modified and extended for production of complex lipids such as GPL (31). *fad23* is orthologous to *fadD26* in *M. tuberculosis*, with 52% amino acid identity and sharing of conserved domains specific to FAAL family proteins. *fadD26* is well described as playing a crucial role in the biosynthesis of complex lipids that populate the outer cell envelope in *M. tuberculosis* (28, 32).

Quantitative PCR of *fadD23* cDNA was compared among serial clinical isolates. We observed significant reductions in the levels of *fadD23* cDNA in the later-collected isolates, suggesting suppressed expression of *fadD23*, potentially leading to reduced synthesis of complex lipids (Fig. 6).

DISCUSSION

In the work-up of cultures for identification and susceptibility testing of MABSC, it is important to note any evidence of mixed populations on the culture plate reflecting a heterogeneous population of in the patient sample. A recent study (35) highlighted this issue by documenting the coisolation of MABSC strains with smooth and rough morphotypes harboring different clarithromycin resistance mechanisms and susceptibility profiles. This work describes additional changes occurring in MABSC over time that may take place prior to noticeable colony morphology changes.

Our results indicate that the rough morphology of *M. abscessus* is associated with the loss of GPL and emerges during chronic, persistent human infection. It should be noted that one of the patients in the study (patient 3) had a disseminated infection due to interferon gamma autoantibodies, the pathophysiology of which is quite different from that of idiopathic bronchiectasis (33). Nevertheless the observed changes in the pathogen genetics and colony morphology in the serial isolates from patient 3 were

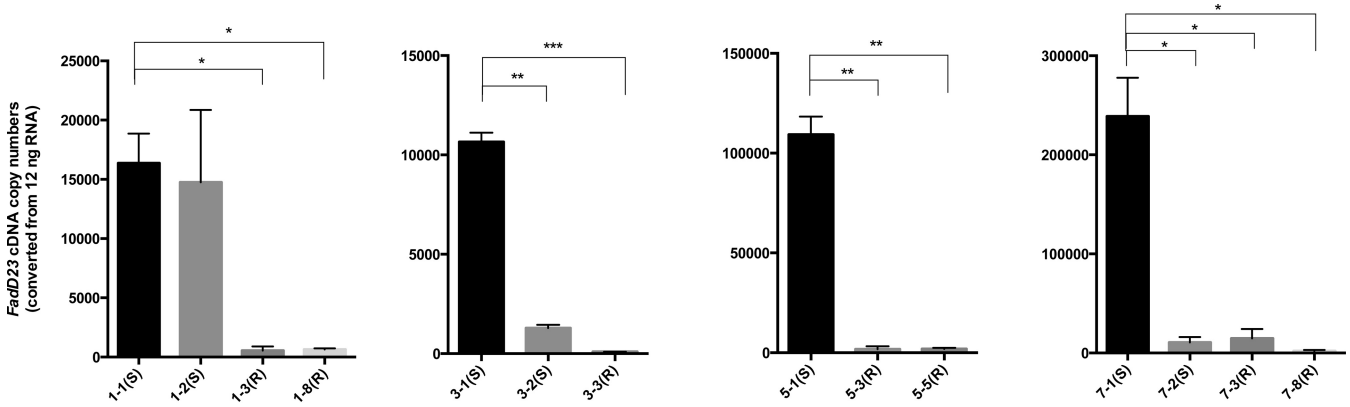

FIG 6 *fadD23* cDNA copy numbers converted from the RNA extracts of isolates from patients 1, 3, 5, and 7. The graphs display the qPCR results from two separate RNA extraction and cDNA conversion experiments for each isolate. A significant reduction in the copy number of *fadD23* mRNA was observed in the later serial isolates. In patients 3 and 7, the reduced expression of *fadD23* occurred even before the appearance of rough morphology. S, smooth; R, rough.

congruent with those for the other patient isolates. Therefore, these changes may not be specific to patients with idiopathic bronchiectasis but may reflect prolonged human infection, treatment, or both.

We identified an underlying genetic change in 77% of rough isolates in this study: spontaneous indels, large deletions, and a nonsense mutation in *mps1-mps2*. These two adjacent genes, likely in one operon, encode nonribosomal peptide synthetases that play indispensable roles in the synthesis of tripeptide-amino alcohol, the core GPL molecule to which fatty acids and complex sugars are attached (9). Inactivating mutations in these genes likely stop GPL synthesis at the very beginning of the pathway. If abandoning GPL production confers selective advantages to the organism in the human environment, as is suggested by our results, it is plausible that isolates with mutations in *mps1-map2* would be selected over others because disrupting *mps1-mps2* may be the most efficient way for the organism to stop GPL synthesis.

Detrimental mutations in *mmpS4-mmpL4a*, found in 13% of the rough isolates, are less obvious than *mps1-mps2* mutations as causes of loss of GPL, due to the paucity of data on these genes. Deshayes et al. (24) deleted *mmpS4* in *M. smegmatis*, thereby causing a switch from smooth to rough morphology, although the mutant was still able to produce a small amount of a "GPL-like molecule." MALDI-TOF MS of the lipid extract from this mutant had a major peak 14 Da higher than that of the wild-type GPL. The authors suggested an additional fatty acid *O*-methylation, the removal of which is dependent on an intact *mmpS4* gene. Interestingly, the same degree of increase in the major peak in MALDI-TOF MS was observed in our spontaneous *mmpS4* mutants compared to smooth clinical isolates. The most plausible explanation is that this molecule is a GPL precursor but probably not able to manifest the phenotypic features of GPL. The morphology of the *mmpS4* mutants was unequivocally rough, and their TLC analysis did not show GPL bands (Fig. 4). The overlapping findings between our results and those of Deshayes et al. (24) imply that *mmpS4* may have a significant role in GPL synthesis.

mmpL4a, on the other hand, has not been studied experimentally. The detrimental mutations found in this gene are uncertain causes of the loss of GPL. We suspect that it has a role in GPL synthesis/transport, based on its adjacency to *mmpL4b* and its apparent indispensability to GPL synthesis (25).

MALDI-TOF MS applications in clinical microbiology have been primarily focused on microbial identification. Our work provides an example of additional applications of the same platform used in the clinical laboratory for the detection of mycobacterial lipid molecules, which unveil adaptive and virulence changes.

We identified different GPL locus mutations among the rough isolates from individual patients (patients 1, 4, 5, 7, and 9) (Table 2), as well as recovered smooth isolates [1-7(S) and 7-6(S)] late in the disease course after several years of recovering only rough isolates. Infection by new strains is less likely, as serial patient isolates were closely related genetically based on our MLST analysis (Fig. 1). More plausible is the coexistence of multiple subpopulations, all diversified from an initial *M. abscessus* strain. Some bacterial subpopulations likely predominate during the course of the infection, hence being more likely to be recovered in culture. Coexistence of diverse lineages has been observed during chronic *Burkholderia dolosa* infection in CF patients (34). Conventional culture and colony selection methods for sputum and bronchoalveolar lavage samples typically yield a predominant strain(s) and likely miss subpopulations occurring simultaneously. Therefore, conventional culture methods could lead to biased results due to lack of information on the collective bacterial population at the time of sputum collection.

There is remarkable variation in rough morphology among the isolates from a single patient, independent of the underlying mutation that led to loss of GPL. Isolates with rough morphology became less defined and structured later in disease in some cases (patients 4, 5 and 6). On the other hand, we found no deleterious mutations in two rough isolates lacking GPL. We postulate that although loss of GPL is sufficient for rough morphology, there may be other genetic changes that cause or affect rough colony morphology.

The accumulation of TAG and the reduced expression of *fadD23*, a gene in the GPL locus involved in activation of fatty acids for synthesis of complex lipids like GPL, were observed in later-collected isolates. On the basis of these findings as well as the similar adaptive changes seen in chronically infective *M. tuberculosis* (26–29), we can hypothesize that *M. abscessus* may gain selective advantages, through yet-unknown mechanisms, from storing fatty acids as TAG instead of using them for synthesis of complex

lipids in the human lung environment. If so, loss of GPL, the most abundant complex glycolipid, could be one of multiple changes that occur under this adaptive process. Accordingly, the absence of GPL alone may not account for the reported pathogenicity associated with rough clinical strains of *M. abscessus*.

ACKNOWLEDGMENTS

This work was supported by the Divisions of Intramural Research of the National Institute of Allergy and Infectious Diseases, the National Heart, Lung and Blood Institute, and the Clinical Center, National Institutes of Health.

We thank the staff members at Outpatient Clinic 11 and the Mycology/Mycobacteriology Section of the Microbiology Department in the National Institutes of Health Clinical Center, whose work had made the serial clinical isolates available for this study.

We declare that we have no conflicts of interest.

REFERENCES

1. **Adekambi T, Reynaud-Gaubert M, Greub G, Gevaudan MJ, La Scola B, Raoult D, Drancourt M.** 2004. Amoebal coculture of "*Mycobacterium massiliense*" sp. nov. from the sputum of a patient with hemoptoic pneumonia. J Clin Microbiol **42:**5493–5501. http://dx.doi.org/10.1128/JCM.42.12.5493-5501.2004.
2. **Adekambi T, Berger P, Raoult D, Drancourt M.** 2006. *rpo*B gene sequence-based characterization of emerging non-tuberculous mycobacteria with descriptions of *Mycobacterium bolletii* sp. nov., *Mycobacterium phocaicum* sp. nov. and *Mycobacterium aubagnense* sp. nov. Int J Syst Evol Microbiol **56:**133–143. http://dx.doi.org/10.1099/ijs.0.63969-0.
3. **Zelazny AM, Root JM, Shea YR, Colombo RE, Shamputa IC, Stock F, Conlan S, McNulty S, Brown-Elliott BA, Wallace RJ, Jr, Olivier KN, Holland SM, Sampaio EP.** 2009. Cohort study of molecular identification and typing of *Mycobacterium abscessus*, *Mycobacterium massiliense*, and *Mycobacterium bolletii*. J Clin Microbiol **47:**1985–1995. http://dx.doi.org/10.1128/JCM.01688-08.
4. **Bryant JM, Grogono DM, Greaves D, Foweraker J, Roddick I, Inns T, Reacher M, Haworth CS, Curran MD, Harris SR, Peacock SJ, Parkhill J, Floto RA.** 2013. Whole-genome sequencing to identify transmission of *Mycobacterium abscessus* between patients with cystic fibrosis: a retrospective cohort study. Lancet **381:**1551–1560. http://dx.doi.org/10.1016/S0140-6736(13)60632-7.
5. **Tettelin H, Davidson RM, Agrawal S, Aitken ML, Shallom S, Hasan NA, Strong M, de Moura VC, De Groote MA, Duarte RS, Hine E, Parankush S, Su Q, Daugherty SC, Fraser CM, Brown-Elliott BA, Wallace RJ, Jr, Holland SM, Sampaio EP, Olivier KN, Jackson M, Zelazny AM.** 2014. High-level relatedness among *Mycobacterium abscessus subsp. massiliense* strains from widely separated outbreaks Emerg Infect Dis **20:**364–371.
6. **Leung JM, Olivier KN.** 2013. Nontuberculous mycobacteria: the changing epidemiology and treatment challenges in cystic fibrosis. Curr Opin Pulm Med **19:**662–669. http://dx.doi.org/10.1097/MCP.0b013e328365ab33.
7. **Jang MA, Koh WJ, Huh HJ, Kim SY, Jeon K, Ki CS, Lee NY.** 2014. Distribution of nontuberculous mycobacteria by multigene sequence-based typing and clinical significance of isolated strains. J Clin Microbiol **52:**1207–1212. http://dx.doi.org/10.1128/JCM.03053-13.
8. **Qvist T, Gilljam M, Jonsson B, Taylor-Robinson D, Jensen-Fangel S, Wang M, Svahn A, Kotz K, Hansson L, Hollsing A, Hansen CR, Finstad PL, Pressler T, Hoiby N, Katzenstein TL, Scandinavian Cystic Fibrosis Study Consortium.** 2015. Epidemiology of nontuberculous mycobacteria among patients with cystic fibrosis in Scandinavia. J Cyst Fibros **14:**46–52. http://dx.doi.org/10.1016/j.jcf.2014.08.002.
9. **Ripoll F, Deshayes C, Pasek S, Laval F, Beretti JL, Biet F, Risler JL, Daffe M, Etienne G, Gaillard JL, Reyrat JM.** 2007. Genomics of glycopeptidolipid biosynthesis in *Mycobacterium abscessus* and *M. chelonae*. BMC Genomics **8:**114. http://dx.doi.org/10.1186/1471-2164-8-114.
10. **Howard ST, Rhoades E, Recht J, Pang X, Alsup A, Kolter R, Lyons CR, Byrd TF.** 2006. Spontaneous reversion of *Mycobacterium abscessus* from a smooth to a rough morphotype is associated with reduced expression of glycopeptidolipid and reacquisition of an invasive phenotype. Microbiology **152:**1581–1590. http://dx.doi.org/10.1099/mic.0.28625-0.
11. **Catherinot E, Clarissou J, Etienne G, Ripoll F, Emile JF, Daffe M, Perronne C, Soudais C, Gaillard JL, Rottman M.** 2007. Hypervirulence of a rough variant of the *Mycobacterium abscessus* type strain. Infect Immun **75:**1055–1058. http://dx.doi.org/10.1128/IAI.00835-06.
12. **Catherinot E, Roux AL, Macheras E, Hubert D, Matmar M, Dannhoffer L, Chinet T, Morand P, Poyart C, Heym B, Rottman M, Gaillard JL, Herrmann JL.** 2009. Acute respiratory failure involving an R variant of *Mycobacterium abscessus*. J Clin Microbiol **47:**271–274. http://dx.doi.org/10.1128/JCM.01478-08.
13. **Jonsson B, Ridell M, Wold AE.** 2013. Phagocytosis and cytokine response to rough and smooth colony variants of *Mycobacterium abscessus* by human peripheral blood mononuclear cells. APMIS **121:**45–55. http://dx.doi.org/10.1111/j.1600-0463.2012.02932.x.
14. **Bernut A, Herrmann JL, Kissa K, Dubremetz JF, Gaillard JL, Lutfalla G, Kremer L.** 2014. *Mycobacterium abscessus* cording prevents phagocytosis and promotes abscess formation. Proc Natl Acad Sci U S A **111:**E943–E952. http://dx.doi.org/10.1073/pnas.1321390111.
15. **Caverly LJ, Caceres SM, Fratelli C, Happoldt C, Kidwell KM, Malcolm KC, Nick JA, Nichols DP.** 2015. *Mycobacterium abscessus* morphotype comparison in a murine model. PLoS One **10:**e0117657. http://dx.doi.org/10.1371/journal.pone.0117657.
16. **Kreutzfeldt KM, McAdam PR, Claxton P, Holmes A, Seagar AL, Laurenson IF, Fitzgerald JR.** 2013. Molecular longitudinal tracking of *Mycobacterium abscessus* spp. during chronic infection of the human lung. PLoS One **8:**e63237. http://dx.doi.org/10.1371/journal.pone.0063237.
17. **Tatham E, Sundaram Chavadi S, Mohandas P, Edupuganti UR, Angala SK, Chatterjee D, Quadri LE.** 2012. Production of mycobacterial cell wall glycopeptidolipids requires a member of the MbtH-like protein family. BMC Microbiol **12:**118. http://dx.doi.org/10.1186/1471-2180-12-118.
18. **Zwadyk P, Jr, Down JA, Myers N, Dey MS.** 1994. Rendering of mycobacteria safe for molecular diagnostic studies and development of a lysis method for strand displacement amplification and PCR. J Clin Microbiol **32:**2140–2146.
19. **Pathak S, Awuh JA, Leversen NA, Flo TH, Asjo B.** 2012. Counting mycobacteria in infected human cells and mouse tissue: a comparison between qPCR and CFU. PLoS One **7:**e34931. http://dx.doi.org/10.1371/journal.pone.0034931.
20. **Bansal-Mutalik R, Nikaido H.** 2014. Mycobacterial outer membrane is a lipid bilayer and the inner membrane is unusually rich in diacyl phosphatidylinositol dimannosides. Proc Natl Acad Sci U S A **111:**4958–4963. http://dx.doi.org/10.1073/pnas.1403078111.
21. **Kuksis A.** 2004. Lipids, p 770–771. *In* Heftmann E (ed), Chromatography: fundamentals and applications of chromatography and related differential migration methods, 6th ed, vol 69B. Elsevier B.V., Amsterdam The Netherlands.
22. **Pawlik A, Garnier G, Orgeur M, Tong P, Lohan A, Le Chevalier F, Sapriel G, Roux AL, Conlon K, Honore N, Dillies MA, Ma L, Bouchier C, Coppee JY, Gaillard JL, Gordon SV, Loftus B, Brosch R, Herrmann JL.** 2013. Identification and characterization of the genetic changes responsible for the characteristic smooth-to-rough morphotype alterations of clinically persistent *Mycobacterium abscessus*. Mol Microbiol **90:**612–629. http://dx.doi.org/10.1111/mmi.12387.
23. **Sonden B, Kocincova D, Deshayes C, Euphrasie D, Rhayat L, Laval F, Frehel C, Daffe M, Etienne G, Reyrat JM.** 2005. Gap, a mycobacterial specific integral membrane protein, is required for glycolipid transport to the cell surface. Mol Microbiol **58:**426–440. http://dx.doi.org/10.1111/j.1365-2958.2005.04847.x.
24. **Deshayes C, Bach H, Euphrasie D, Attarian R, Coureuil M, Sougakoff W, Laval F, Av-Gay Y, Daffe M, Etienne G, Reyrat JM.** 2010. MmpS4 promotes glycopeptidolipids biosynthesis and export in *Mycobacterium smegmatis*. Mol Microbiol **78:**989–1003. http://dx.doi.org/10.1111/j.1365-2958.2010.07385.x.
25. **Nessar R, Reyrat JM, Davidson LB, Byrd TF.** 2011. Deletion of the mmpL4b gene in the *Mycobacterium abscessus* glycopeptidolipid biosynthetic pathway results in loss of surface colonization capability, but enhanced ability to replicate in human macrophages and stimulate their innate immune response. Microbiology **157:**1187–1195. http://dx.doi.org/10.1099/mic.0.046557-0.
26. **Daniel J, Deb C, Dubey VS, Sirakova TD, Abomoelak B, Morbidoni HR, Kolattukudy PE.** 2004. Induction of a novel class of diacylglycerol acyltransferases and triacylglycerol accumulation in *Mycobacterium tuberculosis* as it goes into a dormancy-like state in culture. J Bacteriol **186:**5017–5030. http://dx.doi.org/10.1128/JB.186.15.5017-5030.2004.
27. **Pandey AK, Sassetti CM.** 2008. Mycobacterial persistence requires the

utilization of host cholesterol. Proc Natl Acad Sci U S A **105:**4376–4380. http://dx.doi.org/10.1073/pnas.0711159105.
28. **Shi L, Sohaskey CD, Pfeiffer C, Datta P, Parks M, McFadden J, North RJ, Gennaro ML.** 2010. Carbon flux rerouting during *Mycobacterium tuberculosis* growth arrest. Mol Microbiol **78:**1199–1215. http://dx.doi.org/10.1111/j.1365-2958.2010.07399.x.
29. **Baek SH, Li AH, Sassetti CM.** 2011. Metabolic regulation of mycobacterial growth and antibiotic sensitivity. PLoS Biol **9:**e1001065. http://dx.doi.org/10.1371/journal.pbio.1001065.
30. **Larrouy-Maumus G, Puzo G.** 2015. Mycobacterial envelope lipids fingerprint from direct MALDI-TOF MS analysis of intact bacilli. Tuberculosis (Edinb) **95:**75–85. http://dx.doi.org/10.1016/j.tube.2014.11.001.
31. **Trivedi OA, Arora P, Sridharan V, Tickoo R, Mohanty D, Gokhale RS.** 2004. Enzymic activation and transfer of fatty acids as acyl-adenylates in mycobacteria. Nature **428:**441–445. http://dx.doi.org/10.1038/nature02384.
32. **Simeone R, Leger M, Constant P, Malaga W, Marrakchi H, Daffe M, Guilhot C, Chalut C.** 2010. Delineation of the roles of FadD22, FadD26 and FadD29 in the biosynthesis of phthiocerol dimycocerosates and related compounds in *Mycobacterium tuberculosis*. FEBS J **277:**2715–2725. http://dx.doi.org/10.1111/j.1742-4658.2010.07688.x.
33. **O'Connell ML, Birkenkamp KE, Kleiner DE, Folio LR, Holland SM, Olivier KN.** 2012. Lung manifestations in an autopsy-based series of pulmonary or disseminated nontuberculous mycobacterial disease. Chest **141:**1203–1209. http://dx.doi.org/10.1378/chest.11-0425.
34. **Lieberman TD, Flett KB, Yelin I, Martin TR, McAdam AJ, Priebe GP, Kishony R.** 2014. Genetic variation of a bacterial pathogen within individuals with cystic fibrosis provides a record of selective pressures. Nat Genet **46:**82–87. http://dx.doi.org/10.1038/ng.2848.
35. **Shallom SJ, Moura NS, Olivier KN, Sampaio EP, Holland SM, Zelazny AM.** 12 August 2015. New real-time PCR assays for detection of inducible and acquired clarithromycin resistance in the *Mycobacterium abscessus* group. J Clin Microbiol http://dx.doi.org/10.1128/JCM.01714-15.